



Hydrological and geochemical responses of fire in a shallow cave system



Fang Bian ^{a,b,c,*}, Katie Coleborn ^{b,c}, Ingrid Flemons ^{b,c}, Andy Baker ^{b,c}, Pauline C. Treble ^{b,d}, Catherine E. Hughes ^d, Andrew Baker ^e, Martin S. Andersen ^{a,b}, Mark G. Tozer ^f, Wuhui Duan ^{b,g}, Christopher J. Fogwill ^h, Ian J. Fairchild ⁱ

^a Water Research Laboratory, School of Civil and Environmental Engineering, UNSW Sydney, NSW 2052, Australia

^b Connected Waters Initiative Research Centre, University of New South Wales, Sydney NSW 2052, Australia

^c School of Biological, Earth and Environmental Sciences, UNSW Sydney, NSW 2052, Australia

^d ANSTO, Lucas Heights, NSW 2234, Australia

^e National Parks and Wildlife Service, Bathurst, NSW 2795, Australia

^f NSW Office of Environment & Heritage, Hurstville, NSW, Australia

^g Key Laboratory of Cenozoic Geology Environment, Institute of Geology and Geophysics, Chinese Academy of Sciences, Beijing, China

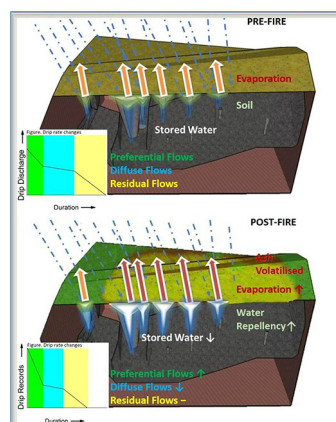
^h Geography, Geology and the Environment, Keele University, UK

ⁱ School of Geography, Earth and Environmental Sciences, University of Birmingham, Birmingham B15 2TT, UK

HIGHLIGHTS

- Severe fire over a shallow cave system leads to changed soil hydrology.
- Cave drip discharge shows increased preferential and decreased diffuse flows.
- Post-fire, stable water isotopes show that soil water was evaporated.
- 6 months post-fire, drip water isotopes have returned to the pre-fire mean.
- Nutrient elements were largely volatilised by the severe fire.

GRAPHICAL ABSTRACT



ARTICLE INFO

Article history:

Received 13 July 2018

Received in revised form 3 January 2019

Accepted 10 January 2019

Available online 11 January 2019

Editor: José Virgílio Cruz

Keywords:

Karst

Fire

Hydrograph analysis

Groundwater

ABSTRACT

The influence of wildfire on surface soil and hydrology has been widely investigated, while its impact on the karst vadose zone is still poorly understood. A moderate to severe experimental fire was conducted on a plot (10 m × 10 m) above the shallow Wildman's Cave at Wombeyan Caves, New South Wales, Australia in May 2016. Continuous sampling of water stable isotopes, inorganic geochemistry and drip rates were conducted from Dec 2014 to May 2017. After the fire, drip discharge patterns were significantly altered, which is interpreted as the result of increased preferential flows and decreased diffuse flows in the soil. Post-fire drip water $\delta^{18}\text{O}$ decreased by 6.3‰ in the first month relative to the average pre-fire isotopic composition. Post-fire monitoring showed an increase in drip water $\delta^{18}\text{O}$ in the following six months. Bedrock related solutes (calcium, magnesium, strontium) decreased rapidly after the fire due to reduced limestone dissolution time and potentially reduced soil CO_2 . Soil- and ash-derived solutes (boron, lead, potassium, sodium, silicon, iodine and iron) all decreased after the fire due to volatilisation at high temperatures, except for SO_4^{2-} . This is the first study to understand the hydrological impact from severe fires conducted on a karst

* Corresponding author at: Water Research Laboratory, School of Civil and Environmental Engineering, UNSW Australia, 110 King Street, Manly Vale, NSW 2093, Australia.
E-mail address: f.bian@unsw.edu.au (F. Bian).

system. It provides new insights on the cave recharge process, with a potential explanation for the decreased $\delta^{18}\text{O}$ in speleothem-based fire study, and also utilise the decreased bedrock solutes to assess the wildfire impacts both in short and long time scales.

© 2019 Published by Elsevier B.V.

1. Introduction

The lack of quantification of the impact of fire events on sub-surface systems, especially in karst environments, limits our understanding of the hydrological impacts of wildfire and the application of prescribed burning on karst geochemistry. The few recent studies examining long-term fire impacts on karst systems focused on changes in soil respiration, nutrient uptake and evaporation associated with the transformation of plant biomass to ash during fire and the subsequent recovery of plant communities (Coleborn et al., 2016b; Nagra et al., 2016; Treble et al., 2016). Coleborn et al., (2016b) compared soil CO_2 concentrations, temperatures and moisture between burnt and unburnt soils at an alpine karst site in Australia. For the first five years, soil respiration was depressed in the burnt forested site and less biomass was reported relative to the unburnt forested site. No significant difference could be seen in the ten-year post-fire soil groups relative to the unburnt control regions. Treble et al. (2016) reported nine-year data on drip water geochemistry, suggesting that the greatest impact of fire is associated with long-term decreases in sulfur concentration, due to post-fire accumulation of this ash-derived nutrient in biomass. Aside from ash signals, higher $\delta^{18}\text{O}$ and chloride levels were associated with increased evaporation in the soil and shallow vadose zone after a wildfire (Nagra et al., 2016). Compared with the bi-decadal time period needed for post-fire habitat and fuel recovery in forest ecosystems (Haslem et al., 2011), soil CO_2 recovery (Coleborn et al., 2016b), and cave drip water isotope, chlorine and sulfur residuals (Treble et al., 2016) are notable in having a multi-year temporal response. In contrast, little is known about the impact of fire on flow regimes, which has the potential to induce short-term fluctuations in response to individual weather events.

Changes in deeper flow regimes may potentially arise as a consequence of widely known impacts of wildfire on soil structures (Fernandez et al., 1999; Pausas et al., 2009; Scott and Van Wyk, 1990). Scott and Van Wyk (1990) reported reduced soil wettability following wildfire. Any influence on soil structures would subsequently affect preferential flow by the modified macropores properties (Beven and Germann, 1982; Ghodrati and Jury, 1992). Cave drip discharge is potentially affected by physical characters such as soil capillarity (Fredlund and Rahardjo, 1993) and preferential flows (Šimůnek et al., 2003). The fire-induced more hydrophobic soil structure can increase post-fire runoff and erosion in burnt areas (Huffman et al., 2001), leading to significant increases in soil loss, and increase in total and quick flow volumes in streams. In cave systems, it potentially modifies the flow regimes with changed drip rate records.

Any surface fire signal transmitted to a cave will pass through the vadose zone—the unsaturated area between the surface and the water tables. In karst environments, the vadose zone hosts the flow pathways and water storages that feed cave drip water, and is where the major processes of bedrock dissolution, mixing and dilution of stored water with event water occur (Fairchild and Baker, 2012). Other hydrochemical and biogeochemical processes along these pathways have also been identified, such as prior calcite precipitation (Fairchild and Treble, 2009), evaporation (Cuthbert et al., 2014) and nutrient and water uptake by vegetation (Coleborn et al., 2016a; Treble et al., 2016). The combination of karst hydrology, water isotope tracers and trace solute mobility are vital for understanding the full complexity of flow pathways (Kogovšek, 2010).

Precipitation percolates through the vadose zone into caves as either *diffuse* or *conduit flows* (Atkinson, 1977). Diffuse flows occur through the matrix porosity, while conduit flows occur via larger scale fractures

or conduits (White, 2002). Relatively lower flow rates and more stable geochemical properties are associated with diffuse flows, while higher and more variable flow rates and more variable chemistry characterise conduit flows. Basic hydrological models of unsaturated zone recharge that include flow rate fluctuations were first developed by Smart and Friederich, 1987. Baker et al. (1997) identified that antecedent precipitation conditions were an important control on the individual hydrological patterns linked to the state of the vadose zone's water storage capacity at the time. Automated acoustic drip counting was recently introduced as an alternative mean of drip recording, which is able to count falling drips, even during transient events, and record small fluctuations in drip rate over several years (Collister and Matthey, 2008). Water isotopes are related to the properties of precipitation (Jouzel et al., 2000) and have been used to distinguish between groundwater and surface water (Sophocleous, 2002), as tracers of moisture sources, and to fingerprint catchment residence times and flow pathways (Tian et al., 2007). In specific regions, the stable isotopes of water ($\delta^2\text{H}$ and $\delta^{18}\text{O}$) can reveal links between climatic factors and flow pathways (Soulsby et al., 2000). The current paper aims to do this for a karst vadose zone.

Solute concentrations in cave drips reflect changes in external forcing (Tremaine and Froelich, 2013) and changes occurring along flow pathways. Multiple lines of evidence are typically crucial in qualitative models of karst vadose zone hydrological behaviour. Theoretically, the Mg/Ca and Sr/Ca ratios are recognized to be important diagnostics in karst hydrology for the amount of prior calcite precipitation and water-rock interaction (Ternan, 1972; Fairchild et al., 2000; Tremaine and Froelich, 2013; Razowska-Jaworek, 2014). Solute abundances vary in response to differences in climate and cave controls (Wassenburg et al., 2012), the type of bedrocks (Immenhauser et al., 2007) as well as the duration of each recharge event (Huang and Fairchild, 2001). Hartland et al. (2012) reported a correlation between natural organic matter-transported metals and climatic signals. Inversely, the quantity of soil organic matter can also be indicated by shifts in the metal ratios of cave drip discharges. Nagra et al. (2016) compared a burnt cave with a nearby control cave. Biomass-sourced, ash-derived solutes (SO_4 and K), together with dissolved bedrock solutes, were both reported as a fire signature. However, it is important to note that drip water solute concentrations can vary significantly even within the same cave chamber (Fairchild and Treble, 2009).

In this research, we aimed to identify the hydrological and geochemical impact of an experimental fire on a shallow karst vadose zone. The fire was deliberately lit above a cave in order to monitor its impact under controlled conditions. We analysed the composition of cave drip water over 2.5 years (Dec 2014–May 2017) in Wombeyan Cave, a shallow cave system in NSW, Australia. Our monitoring started 1.5 years prior to the fire and continued for one year afterwards. Thus, unlike the previous studies by Nagra et al. (2016) and Treble et al. (2016), which contain only post-fire data, this study also includes pre-fire data to serve as a baseline with which post-fire data may be compared. This greatly assists in our attempts to understand and quantify the impacts of fire on karst systems. This is the first published research to directly compare pre- and post-fire hydrogeochemical components and drip discharges in a shallow karst vadose zone after a severe fire. Reports of pre- and post-fire discharge patterns and water stable isotopes were made to demonstrate changes to the local vadose zone's hydrology, while inorganic geochemical changes were also analysed as supplementary evidence. It is therefore valuable to directly compare pre- and post-fire hydrogeochemical components and drip discharge for commonalities and differences.

2. Site description

The Wombeyan Caves Karst Conservation Reserve (34° 18' S, 149° 58' E) is located in the south-eastern part of New South Wales, Australia, on the western edge of the Sydney Basin, on a plateau of the Great Dividing Range, surrounded by agricultural areas (Fig. 1). Wombeyan Limestone, part of the Bungonia Group, is now a marble due to the formation of igneous rocks in the surrounded Lower-Middle Devonian Bindook Porphyry Complex (Brunker and Offenber, 1970; Osborne, 1984). These Silurian carbonates are highly fractured marbles with no matrix porosity remaining (Osborne, 1993). Therefore, flow is entirely dominated by fracture and conduit flows. Typically, the land surfaces (<4 cm depth) above the caves contain gravel, marble fragments, red silty clay and dark humic matter (McDonald and Drysdale, 2007).

The mean monthly land-surface temperature at Wombeyan Caves ranges between a maximum of 26.0 °C in January to a minimum of 0.6 °C in July. Annual median long-term precipitation is 684.7 mm (1942–2017, from Bureau of Meteorology, Australia gauge 063093), with summer precipitation exceeding winter precipitation by 47%. However, during December 2014 to May 2017, winter monthly precipitation (104 mm) exceeded that of summer by 32% (79 mm).

Wildman's Cave (W456) is a small and shallow cave near the top of a ridge above Mares Forest Creek Gorge. The cave has a narrow pothole-type entrance and 42 m of reasonably decorated passage (Wylie and Wylie, 2004). The single large chamber is approximately 15 m long and 6 m wide, with <1 m of soil and bedrock overlying the cave.

3. Method

3.1. Experimental fire

An experimental fire covering an area of 10 m × 10 m was conducted above Wildman's Cave on 25th May 2016. Given the

experimental nature of the fire, additional fuel (branches and leaf litter collected adjacent to the site) was placed within the burn area to ensure that a moderate to severe intensity burn was achieved. Within the 10 m × 10 m burn area, shrubs and groundcovers dominated the site. There were no mature trees within the burn site.

3.2. Location of monitoring sites within the cave

Eleven dripping stalactites in Wildman's Cave were included in this study to monitor the geochemical and hydrological variations associated with the burn (see Fig. 1b). In the corner of the pothole-type entrance, a straw stalactite (Site 01) was utilised (see Fig. 1b). A large cluster of soda-straws separated the entrance from the inner chamber, and provided drips for Sites 02 to 05. Sites 06 to 11 were located within the large chamber, while Sites 02 to 05 were a lower elevation than the others and had a thicker roof.

3.3. In-cave water sampling

In-cave monitoring started in Dec 2014 and ended in May 2017. Water samples were collected at approximately bi-month intervals throughout the research program, with sample volumes limited by the infrequent occurrence of recharge events. Two drip water sampling methods were employed. Firstly, drip water samples were collected by leaving bottles in the cave for approximately two months. Wide-mouth 120 ml HDPE sampling bottles were placed under each dripping site, with a plastic funnel containing an acoustic data logger placed inside. Each of these bottles used for cumulative drip water sampling contained 2 mm paraffin oil layer to prevent evaporation or exchange with the atmosphere once drips entered the sampling bottle. Secondly, opportunistic sampling was conducted during each of the bi-monthly sampling campaigns, provided recharge was occurring. These drip waters were sampled directly into 250 ml wide-mouth HDPE sampling bottles placed directly under the drip sites overnight. The collection of

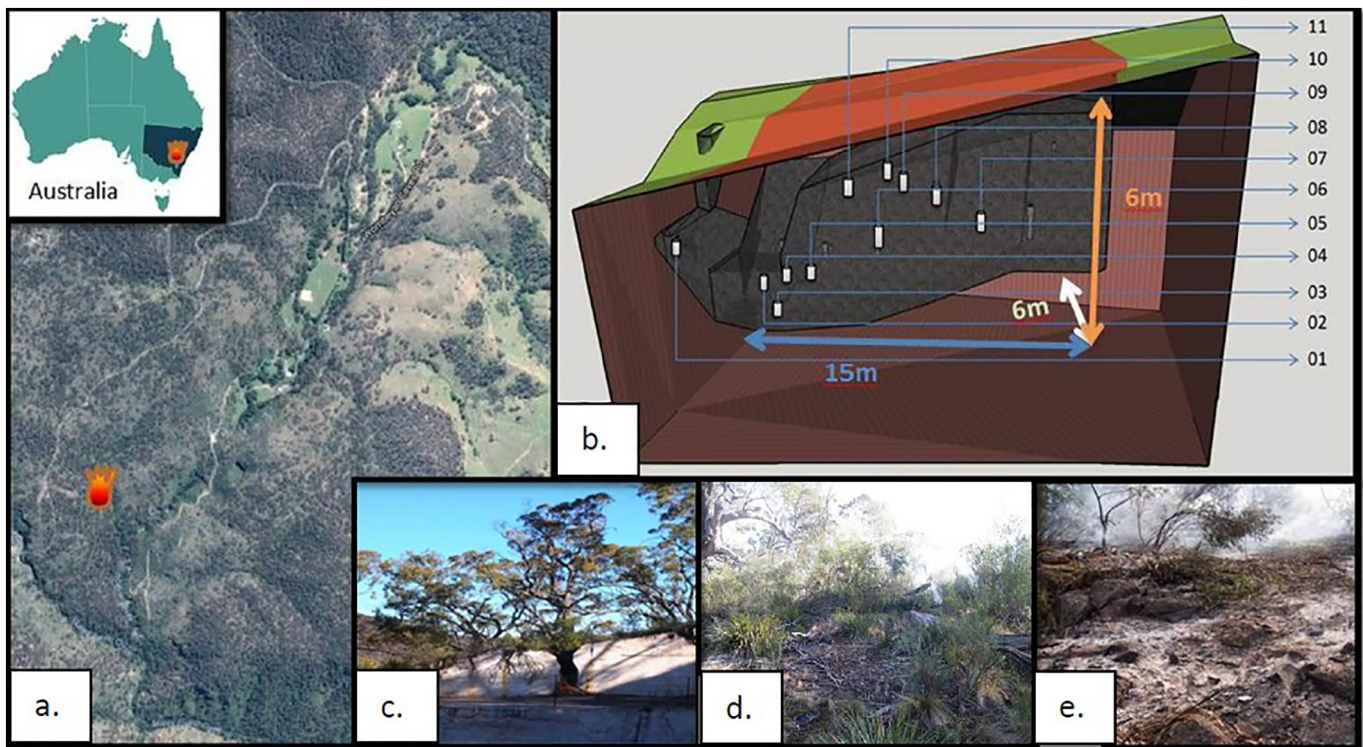


Fig. 1. Location of Wildman's Cave Conservation Reserve in Wombeyan Caves, New South Wales, Australia (a), 3D diagram of the study site. Recorded sites are indicated with white rectangles (b), exposed Wombeyan limestone (c), burnt area pre-fire (d) and post fire (e). Photo (a): Google Earth. Photos (c, d and e): Andy Baker.

these campaign samples was conducted without funnels or drip loggers to minimise contamination from the surrounding environment. Reference groundwater samples were collected from a local borehole in the Wombeyan Caves campground using 250 ml wide-mouth HDPE containers. Sixty-two opportunistic samples were collected when the cave was dripping during the bi-monthly sampling campaigns. There were fewer samples collected in the dry cold months, especially after fire. At the day after the fire we succeeded in acquiring ten drip samples the day, then six more in the first month. After that, water samples were collected in Dec 2016, and Jan and Mar 2017. Bore hole samples were collected using 250 ml wide-mouth HDPE containers in Wombeyan Caves.

3.4. Precipitation

Wombeyan monthly rainfall records were provided via Bureau of Meteorology climate station (Number. 063093). Precipitation samples for stable water isotopes analysis were collected from Mount Werong (34° 04' S, 149° 55' E), which was the nearest precipitation isotope collection station to Wildman's Cave (~30 km to the northeast). Precipitation samples were collected on an event basis using a sealed HDPE bottle with a plastic funnel. The design was based on the method of Gröning et al. (2012) in order to prevent evaporation of the sample or isotopic exchange with the atmosphere. The rainfall-related collection here was from August 2014 to May 2017, and is an extension of a time series previously published by Hughes and Crawford (2013) and further described by Crawford et al. (2013).

3.5. Drip hydrology monitoring

Hydrology records were comprised of drip rates from stalactites within the cave, which were integrated at 15-min intervals using acoustic drip loggers (Stalagmate® Plus Mk 2b, <http://www.driptych.com/>). For each drip site, a Stalagmate was placed underneath the stalactite in a plastic funnel sitting in an HDPE bottle surrounded by a plastic tube to fix it in position. The minimum distance between the stalactite and Stalagmate was 25 cm. The volume of drips was assumed to be consistent throughout this study (Collister and Matthey, 2008).

3.6. Geochemical analysis

Both the long-term and short-term drip water samples collected were first filtered through 0.45 µm mixed-cellulose filters into 10 ml plastic sampling vials. Water samples for stable isotope analysis were stored in 10 ml vials with zero-headspace. Separate 10 ml vials were used for solute analyses. Two drops of ACS reagent HNO₃ acid (70%) were added into the cationic samples to prevent precipitation. All the prepared analytes were refrigerated at <5 °C until analysis.

Dripwater samples were analysed to determine the δ²H and δ¹⁸O, with the results given in per mille (‰) using the conventional delta notation relative to VSMOW (Vienna Standard Mean Ocean Water). A Los Gatos Research (LGR) Water-Vapour Isotope Analyzer in the UNSW IceLab was used for the analysis of the δ²H and δ¹⁸O. The ICELAB was graded excellent in an international inter-laboratory comparison prior to the period of sample analysis (Wassenaar et al., 2018). All the isotope analytes were filtered through 0.45 µm mixed-cellulose filters again before injection into the isotope analyzer (reported accuracy of ±1.0‰ for δ²H and ±0.2‰ for δ¹⁸O). The samples were calibrated against five standards, with VSMOW-2 run as a primary standard. Some 109 precipitation samples were analysed at the ANSTO Environmental Isotope Laboratory using a Picarro L2120-I Water Analyzer (same accuracy as the LGR Water-Vapour Isotope Analyzer). The ANSTO lab runs a minimum of two in-house standards calibrated against VSMOW/VSMOW2 and SLAP/SLAP2 with samples in each batch. Deuterium excess (D-excess) is calculated with the equation $d = \delta^2\text{H} - 8 * \delta^{18}\text{O}$.

Only opportunistic over-night collections of water samples were analysed for cations and anions. Cation (B²⁺, Ba²⁺, Ca²⁺, Fe²⁺, K⁺, Mg²⁺, Na⁺, Pb³⁺, Si⁴⁺ and Sr²⁺) concentrations were determined using inductively-coupled plasma optical emission spectroscopy (ICP-OES; Optima™ 7300DV, PerkinElmer, Shelton, USA) and inductively-coupled plasma mass spectrometry (ICP-MS; NexION 300D, PerkinElmer, Shelton, USA) at the UNSW Mark Wainwright Analytical Centre, except for water samples from the final collection (9th May 2017), which were analysed using inductively-coupled plasma-atomic emission spectroscopy (ICP-AES; ICAP7600, Thermo Fisher) at the Australian Nuclear Science and Technology Organisation (ANSTO). Anion (Cl⁻, I⁻ and SO₄²⁻) concentrations were determined using an ion chromatograph (Dionex DX-600) with a self-regenerating suppressor at the ANSTO facility. Mann-Whitney *U* tests (Mann and Whitney, 1947) were conducted on cation and anion as a non-parametric test for the geochemistry data which were not normally distributed over 2 years. *U* and *Z*-scores are calculated with the equations:

$$U = R - \frac{n(n+1)}{2}, z = \frac{U-m}{\sigma}$$

where *n* is the sample size, *R* is the sum of the ranks, *m* and σ are the mean and standard deviation of *U*. The *U*-score allows the comparison of different groups. The *Z*-score permits the comparison of the standard normal quantiles to obtain the calculated probability

4. Results

4.1. Experimental fire

The highest recorded temperature was 929 °C in the middle of the burn area at 12 cm depth (Supplementary Fig. 1) recorded using a thermocouple temperature recorder TCTemp1000 (Thermoworks™). The fire intensity was severe (Keeley, 2009), with canopy cover left intact but the surface litter largely consumed and thick white ash layers generated at hotspots to a depth of several centimetres. The fire was started mid-morning, and visible flame lasted approximately 45 min.

4.2. Hydrology results

The overall drip water recharge responses to precipitation are illustrated in Fig. 2. Site 03 slowly stopped dripping, while Sites 08–10 were misaligned post fire. 14 major drip water recharge events occurred pre-fire, and 21 major drip water recharge events occurred post fire. For periods outside of the recharge events dripping ceased (e.g. the baseline drip logger signals were constantly 0). Comparing the number and timing of recharge events to daily precipitation data, a recharge threshold of about 20 mm/day precipitation is inferred. In the 18-month pre-fire monitoring period, there were 10 days where daily precipitation exceeded 20 mm, with precipitation exceeding 50 mm/day on one of these occasions. In the 12-month post-fire monitoring period, there were 11 days where daily precipitation exceeded 20 mm, including precipitation exceeded 50 mm/day on two occasions. The highest daily rainfall total over the monitoring period (91.4 mm) occurred one week after the fire. Despite minor differences in pre- and post-fire daily rainfall amounts, Fig. 2 shows a notable change in the drip pattern after the fire.

The descriptive statistics for basic parameters, including duration, peak rates, average rates, total drips, skewness and kurtosis for all individual recharge events are presented in Fig. 3, which uses box plots to compare discharge patterns pre- and post-fire. Post-fire total drips were less variable but not significantly different to pre-fire total drips. Both peak and average recharge rates increased noticeably and were associated with decreased duration after the fire. Detailed analyses of the event hydrographs are presented in Section 5.1. Overall, post-fire discharge events were characterised by higher mean and peak flows that

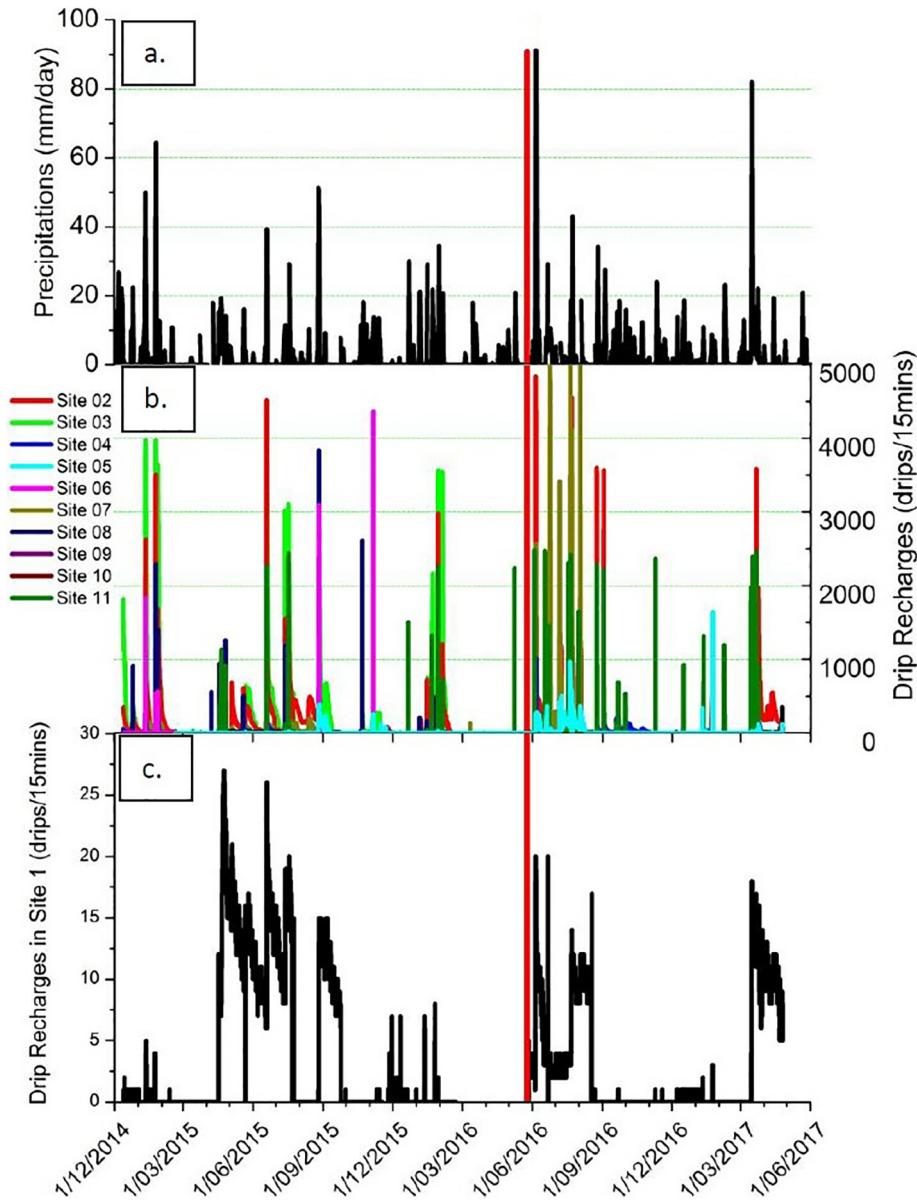


Fig. 2. Precipitation records at Wombeyan Caves (a), compared with the overall discharge into the cave at burnt drip sites (b) and Site 01 (c). Discharge records at individual sites are presented using the colour in agreement with subsequent figures. The timing of the fire is indicated by the vertical red line. Records on individual sites could be found in Supplementary Fig. 2.

were of shorter duration than pre-fire discharge events. Increased peak recharge was observed at Sites 02, 04, 05, 07, 09 and 11 (Supplementary Fig. 2) two weeks post-fire. The skewed discharge peaks were shorter for post-fire recharge events than pre-fire ones. Conversely, there were no notable changes in dripping pattern for Site 01, which was not directly under the burnt area (Supplementary Fig. 2).

4.3. Isotope results

Isotopic data for the 184 precipitation events collected at Mt. Werong from August 2014 to May 2017 (January 2015 was missing due to insufficient rainfall) show that the values for $\delta^{18}\text{O}$ ($n = 166$) ranged from -17.7‰ to 3.1‰ , and from -126.4‰ to 31.6‰ for the $\delta^2\text{H}$ samples ($n = 184$). The weighted mean of precipitation were isotopically higher in the 12 months pre-fire ($\delta^{18}\text{O} = -6.3\text{‰}$, $\delta^2\text{H} = -31.6\text{‰}$) than the 12 months post-fire ($\delta^{18}\text{O} = -7.9\text{‰}$, $\delta^2\text{H} = -48.2\text{‰}$).

Post-fire, in June 2016, the lowest isotope values were observed, and when a prolonged period of rain occurred at both Mt. Werong and Wombeyan Caves, where 238 mm fell over 22 rain days, more than three times the long-term mean precipitation for June (69.9 mm). This was associated with two consecutive eastcoast low-pressure systems affecting the NSW coast in one month, resulting in record high daily and monthly rainfall records at many stations. The rain from these two systems was significantly isotopically lower, with a monthly $\delta^{18}\text{O}$ mean of -14.5‰ and a $\delta^2\text{H}$ mean of -98.7‰ in June 2016.

Drip water $\delta^{18}\text{O}$ values for 213 samples are presented in Fig. 5 which were controlled by the precipitation conditions and residual time in the flow paths (Cuthbert et al., 2014; Jouzel et al., 2000). Until May 2016, $\delta^{18}\text{O}$ values ranged from -8.5‰ to -3.1‰ , and $\delta^2\text{H}$ values ranged from -50.6‰ to -10.1‰ . After the fire, sites behaved differently according to their locations (See Fig. 1b). For the shallower sites (Sites 07–11), there was a response the day after the burn, with the mean $\delta^{18}\text{O}$ values being 4.5‰ lower than that for all pre-fire samples

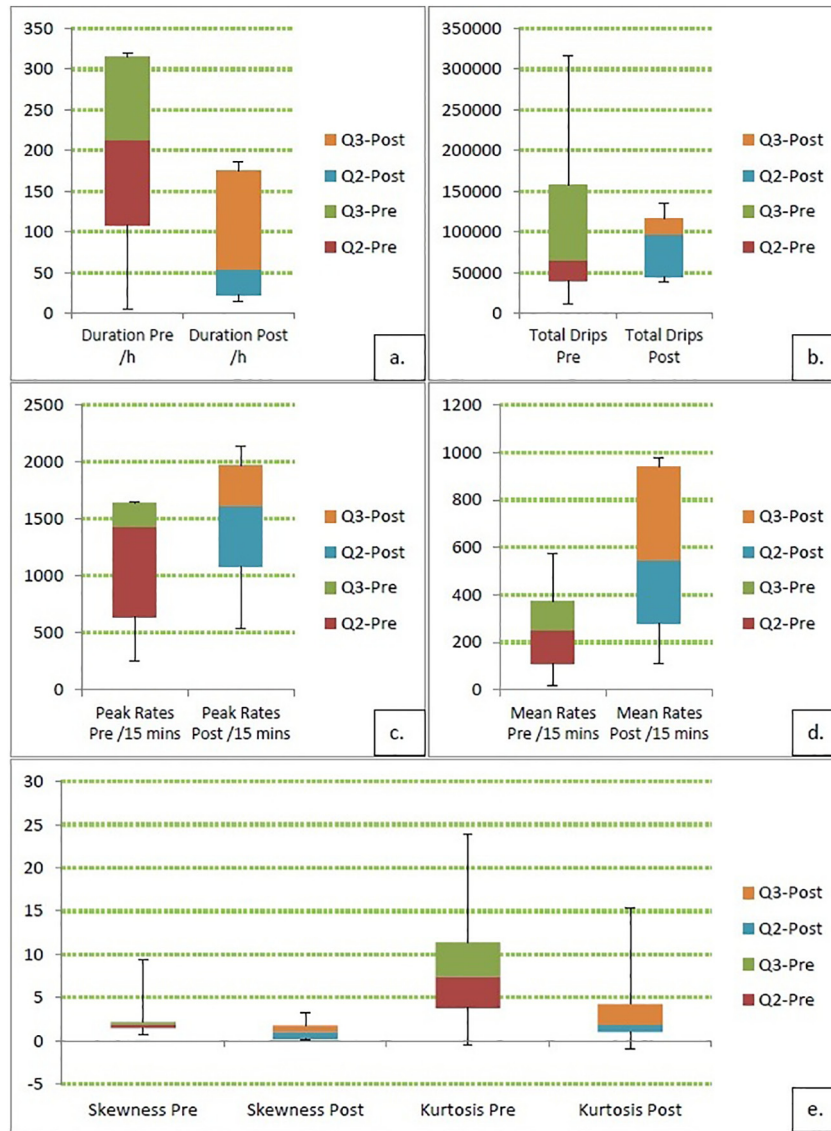


Fig. 3. Box plots of descriptive statistics for all individual recharge events at the drip sites below the burnt site: duration (a), peak drip rates (b), mean drip rates (c), total drip amount (d), and skewness and kurtosis (e). Q2 and Q3 are shaded and represent the second and third Quartiles (the inter-quartile range). First and fourth quartiles are indicated via the whiskers.

(−5.1‰ to −9.6‰). In contrast, there was only a slight difference in $\delta^{18}\text{O}$ at Sites 02–06 (−5.5‰ to −6.2‰).

The largest shift occurred during the next sampling campaigns (5 and 21 June 2016). All isotopic values of the ten burnt sites were significantly lower (−76.5‰ and −84.1‰ in $\delta^2\text{H}$ for Sites 02–06 and 07–11, respectively, and −11.9‰ and −12.7‰ in $\delta^{18}\text{O}$). One month later, the sites showed a return trend to the pre-fire average until a new peak was reached in March 2017. The isotopic values of Site 01 were consistently lower than its pre-fire mean values. After December 2016, drips at the Site 1 were isotopically lower than those at the burnt sites. Over the post-fire hydrological year, drip water became more isotopically depleted than that pre-fire.

Comparison of drip water and precipitation D-excess identifies a higher D-excess in the drip waters compared to precipitation pre-fire. D-excess for drip waters and precipitation are more similar immediately post-fire. This lower D-excess verified that the fire depleted the stores, such that old water which would have been affected by evaporation was removed by the fire and the stores were replenished with new recharge (Froehlich et al., 2008).

The pre-fire drip water stable isotope composition was above the global meteoric water line (GMWL; Fig. 6). The local meteoric water

line (LMWL) was established using precipitation data from Mt. Werong. Three different groups based on their spatial locations in the cave were plotted separately in Fig. 6a and b. In Fig. 6a, the slope for Sites 07–11 (slope = 6.5 ± 0.4) was similar to the LMWL (slope = 6.6 ± 0.3), and Site 01 (slope = 5.8 ± 1.4). Three groundwater samples from the borehole in Wombeyan camping area were collected, on 23 September 2015, 11 Jan and 23 March 2017, and had an average $\delta^2\text{H}$ of -38.45 ± 5.10 ‰ and an average $\delta^{18}\text{O}$ value of -7.31 ± 0.59 ‰ (Fig. 5, shaded blue).

4.4. Solute results

The solutes showed great variability between sites. Results of Mann-Whitney *U* tests showed there was a significant difference between different time periods for some drip water solute concentrations (Table 1, and the time series for individual solute in Supplementary Fig. 4). The concentrations of all bedrock-derived solutes in drip water (Ca^{2+} , Mg^{2+} and Sr^{2+}) were significantly lower after the fire. Barium did not change immediately but decreased after six months. The decreases in concentrations of Ca^{2+} , Mg^{2+} and Sr^{2+} were substantial one month post-fire and partially

Table 1
Descriptive statistics and Mann-Whitney *U* test results for solute concentrations. Samples are separated into three groups (pre-fire, 1 month post-fire and 6 months post-fire). Statistical significance ($p < 0.05$) is indicated in bold text. Z-scores represent the number of standard deviations between each data point and the mean.

Ion	Sampling Time	Number	Min	Quartile 1	Median	Quartile 3	Max	<i>U</i>	<i>Z</i>	Exact prob> <i>U</i>
B ²⁺ /μg·L ⁻¹	Pre-fire	7	4.9	11.6	27.4	33.3	62.4			
	1 mth post-fire	15	2.2	3.5	5.0	10.2	14.4	95.0	3.0	0.0
	6 mth post-fire	10	2.0	2.0	2.0	4.3	6.0	94	2.2	0.0
Ba ²⁺ /mg·L ⁻¹	Pre-fire	12	1.4	3.9	4.4	6.4	23.3	–		
	1 mth post-fire	13	1.6	2.3	3.0	12.8	30.1	105	1.4	0.2
	6 mth post-fire	10	2.0	2.0	2.0	4.3	6.0	94	2.2	0.0
Pb ³⁺ /μg·L ⁻¹	Pre-fire	14	0.0	0.0	0.1	0.2	0.2			
	1 mth post-fire	15	0.0	0.0	0.0	0.1	0.1	147.5	1.8	0.1
	6 mth post-fire	10	0.0	0.0	0.0	0.1	0.1	147.5	1.8	0.1
Ca ²⁺ /mg·L ⁻¹	Pre-fire	40	47.0	87.2	107.9	119.1	150.5	–		
	1 mth post-fire	14	49.4	57.1	65.8	74.4	81.9	525	4.8	0.0
	6 mth post-fire	10	67.9	75.4	91.8	99.8	110.0	288	2.1	0.0
Mg ²⁺ /mg·L ⁻¹	Pre-fire	29	0.4	0.8	1.3	1.5	2.3	–		
	1 mth post-fire	14	0.6	0.7	0.7	0.8	1.4	311	2.8	0.0
	6 mth post-fire	10	0.7	0.8	1.1	1.2	1.6	179	1.1	0.3
Sr ²⁺ /μg·L ⁻¹	Pre-fire	38	1.4	61.4	72.5	84.5	109.4	–		
	1 mth post-fire	13	0.2	36.2	40.1	71.7	78.9	384	3.0	0.0
	6 mth post-fire	10	37.0	46.8	50.5	57.8	64.0	10	3.5	0.0
Na ⁺ /mg·L ⁻¹	Pre-fire	20	1.1	1.6	1.8	2.0	2.6	–		
	1 mth post-fire	14	1.0	1.2	1.4	2.0	2.0	190	1.7	0.1
	6 mth post-fire	10	1.1	1.2	1.3	1.9	2.5	142	1.8	0.1
Cl ⁻ /mg·L ⁻¹	Pre-fire	27	1.2	2.5	3.1	4.0	11.6	–		
	1 mth post-fire	14	2.1	2.7	4.5	6.7	13.1	12	–1.5	0.1
	6 mth post-fire	10	2.7	2.9	3.7	6.5	14.0	101	–1.2	0.3
K ⁺ /mg·L ⁻¹	Pre-fire	21	0.1	0.6	0.8	3.0	25.2	–		
	1 mth post-fire	14	0.1	0.1	0.4	1.0	1.5	218	2.4	0.0
	6 mth post-fire	10	0.1	0.1	0.2	0.3	1.2	190	3.6	0.0
Si ⁴⁺ /mg·L ⁻¹	Pre-fire	39	1.0	1.5	2.0	2.0	2.3	–		
	1 mth post-fire	14	1.0	1.1	1.2	1.3	1.4	516	4.9	0.0
	6 mth post-fire	10	1.2	1.4	1.5	1.6	1.8	303	2.7	0.0
I ⁻ /mg·L ⁻¹	Pre-fire	19	0.1	0.1	0.3	1.5	7.3	–		
	1 mth post-fire	8	0.1	0.5	1.0	1.3	1.5	61	–0.8	0.4
	6 mth post-fire	10	0.1	0.1	0.1	0.1	0.1	180	4.0	0.0
SO ₄ ²⁻ /mg·L ⁻¹	Pre-fire	27	0.0	0.1	0.1	0.2	0.4	–		
	1 mth post-fire	14	0.3	0.4	1.2	6.2	20.6	3	–5.1	0.0
	6 mth post-fire	10	0.4	0.6	0.8	1.4	2.6	0	–4.6	0.0
Fe ²⁺ /mg·L ⁻¹	Pre-fire	35	0.6	1.5	2.0	2.8	5.5	–		
	1 mth post-fire	14	0.9	1.1	2.0	3.2	9.7	243	0.0	1.0
	6 mth post-fire	6	0.0	0.0	0.0	0.0	0.0	210	3.9	0.0

recovered six months post-fire. Chloride remained lower after the fire. Sulphate increased 10-fold one month post-fire and although it decreased between one and six months post-fire, it remained above pre-fire levels. Iodide slightly increased initially, but returned to below the pre-fire level half a year later.

5. Discussion

5.1. Changes in cave drip hydrology and Karst architecture

By comparing log₁₀-transformed changes in drip rates over time (see Supplementary Fig. 3), the drainage stages during the recession stage of individual recharge events can be identified. These stages are represented conceptually in Fig. 7. Through the changes of the slopes (the log₁₀-transformed rates of decrease in recharge), we can interpret the changes to the dominant recharge flow patterns at each site. Three different stages in the recession stage of recharge for individual precipitation events are identified.

- In the first stage of recession (Fig. 7, green), when both the soil and karst are saturated with event water, soil moisture is above field capacity, which permits the maximum possible recharge rate from the soil to the karst stores. The major pathway for the event water is through preferential paths in the surface soil directly to the karst fractures, with bypass or overflow of the karst stores. Flow rates are mainly restricted by the minimum diameter of the fracture in the karst, or the internal diameter of the stalactite.
- In the second stage (Fig. 7, blue), the soil is no longer saturated enough to support preferential flow in the soil and overflow or

bypass flow in the karst. Soil diffuse flow from the soil into the karst stores becomes the dominant flow pathway. In this way, relatively slower recharge rates from the soil, and longer residence time in karst stores, generate lower slopes. In some cases, especially in the inner part of the cave like Site 07, this stage is less frequently observed or even mixed with the first stage. We hypothesise that this is due to lower soil water storage volumes and weaker capillarity effects from a thinner soil layer.

- In the final stage (Fig. 7, yellow), when the surface precipitation has stopped and soil moisture falls below field capacity, drainage to the karst by soil diffuse flow also stops. The amount of new event water is now low. The cave drips are quickly recharged from the residual karst stores, and the drip rate is again limited by the diameters of the fractures or stalactites.

There is no sign of any original sedimentary structures in the Wombeyan Limestone as it is formed of marble and therefore it effectively contains only secondary porosity. Preferential flow in the soil and overflow or bypass flow in the karst dominates cave recharge in Wildman's Cave. Theoretically, discharge from soil storage would be buffered by soil capillarity (Fredlund and Rahardjo, 1993) resulting in moderate drip rates and soil diffuse flows to the karst and cave below. When there is no interaction between the soil water store and the bedrock, discharge only occurs from the karst water store and drip rate peaks are likely to decline more rapidly.

Fires can change the physical and chemical properties of soil (Bonacci et al., 2008). Post-fire, with low soil water content and high

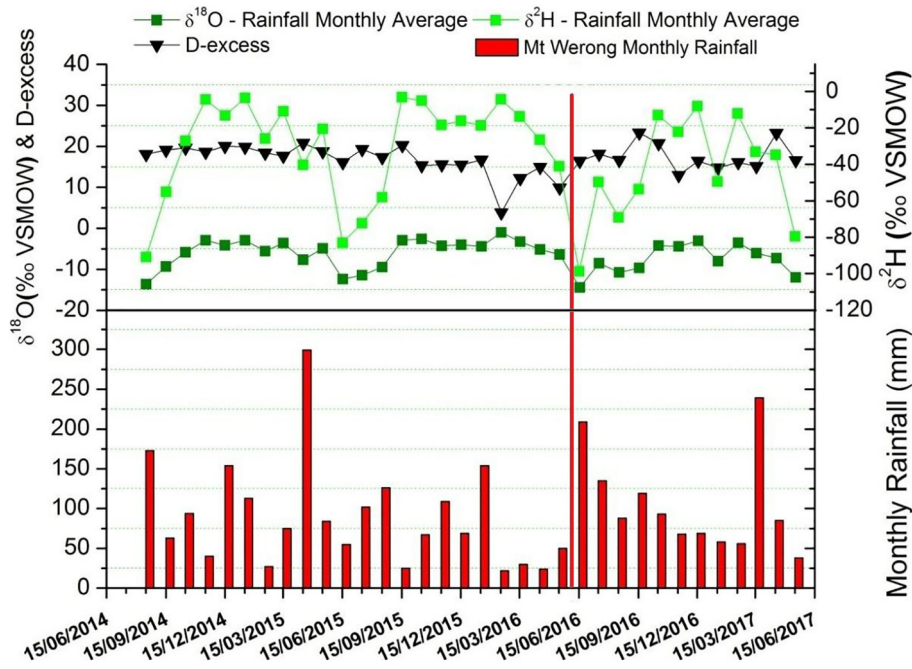


Fig. 4. Monthly weighted mean rainfall at Mt. Werong comparing to recorded rainfall amounts. Rainfall D-excess is also displayed. The vertical line indicates the timing of the experimental fire (25th May 2016 indicated by the red line).

air saturations, the relative permeability to water is negligible. Therefore soil diffuse flow should be severely reduced after the fire, at least initially (Russo, 1998). Immediately post-fire, in an initially gas saturated soil, part of the first recharge will be consumed to fill the capillary reservoir, and will therefore not contribute to the flow recorded in the cave drips. An increase in soil hydrophobicity can affect flow paths within the soil (Huffman et al., 2001). Stoof et al. (2014) reported that fire-induced preferential flows are associated with a change in soil water repellency. Plaza-Álvarez et al. (2018) also reported the increased soil water repellency after prescribed burns in forest ecosystems, and a recovery trend was monitored. The total storage volume is unchanged post-fire, with similar total recharge amounts pre- and post-fire (see Fig. 3c). The post-fire recharge in Wildman's Cave was more intense, having a higher magnitude, shorter duration and less frequent

hydrographic peaks than the pre-fire recharge. Hereby, a post-fire increase in preferential flow in the soil could explain the observed change in drip rates in the three stages described in Fig. 7.

Three effects of fire on the recession stages (arrows in Fig. 7) are described below:

Effect 1) For the deeper sites, which were covered with a thicker soil layer (Sites 02–04), A Model predict increases in mean post-fire drip rates for all precipitation events across all the stages of recession. The peak flow rates increased slightly. Fire-induced increases in soil preferential flow pathways increased the drip rates in the stage a green. In the second stage, an increase in soil hydrophobicity weakened the soil's capillary action, which substantially decreased the duration of the soil

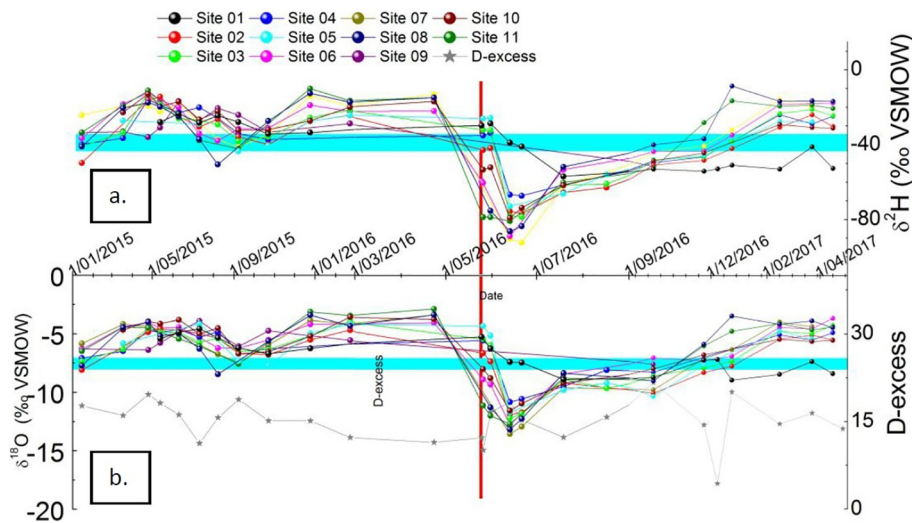


Fig. 5. $\delta^2\text{H}$ (a), $\delta^{18}\text{O}$ variations and D-excess (b) of drip water from 01/01/2016 to 01/01/2017. The experimental fire is indicated by the red line. Horizontal blue band represents the mean isotope values for local groundwater: $\delta^2\text{H} = -38.45\text{‰} \pm 5.10\text{‰}$, $\delta^{18}\text{O} = -7.31\text{‰} \pm 0.59\text{‰}$. The x-axis scale is expanded for the period 01/03/2016 to 1/09/2016 to better show the post-fire isotope data.

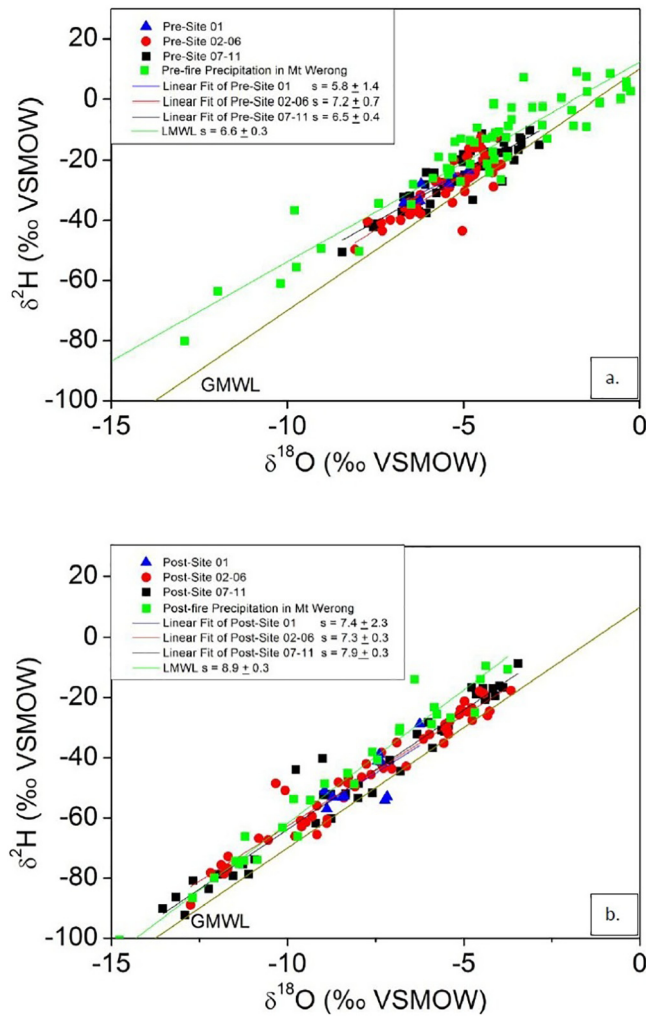


Fig. 6. $\delta^2\text{H}$ and $\delta^{18}\text{O}$ data for pre-fire (a) and post-fire samples (b).

diffuse flow controlled stage. In the final recession stage, the karst stores were unaffected by the surface fire, and there was no change in the draining of the last water from the fractures.

- Effect 2) For the shallower sites (Site 07), B Model describes the amplified effects of changes in soil hydrophobicity and preferential flows. At Site 07, soil diffuse flow was the dominant process pre-fire, and the preferential flows were not obvious. Post-fire, newly created preferential flows dominated the soil diffuse flows, so that the drip rate for this site was mainly controlled by the first stage.
- Effect 3) For sites in the middle part of the cave, deeper than Site 02 and with a thinner soil layer than Site 01 (e.g. Site 05), there was a similar pre-fire drip rate A Model to that at Sites 02–04. Increased preferential flows dominated the soil diffuse flows which originally appeared in the second stage.

Both Sites 06 and 11 were fed by two asynchronously dripping stalactites, making it difficult to identify the specific stages (See Supplementary Fig. 3). However, increased preferential flows possibly still occurred at both sites. Overall, we propose that the fire-induced increase in preferential flows and the loss of soil capillarity both led to more intense cave drip recharge.

5.2. Stable isotope behaviour and residence time of drip waters

Fig. 4 showed that Wildman's Cave drip water $\delta^2\text{H}$ and $\delta^{18}\text{O}$ values were less variable than the values for Mt. Werong precipitation, indicative of mixing of water in the soil and karst. Figs. 4 and 5 above show that the variability in drip water isotopic composition broadly follows that of precipitation, albeit damped and lagged. Post fire, drip water stable isotope composition has a negative isotopic excursion following a high magnitude (164.0 mm over three days), isotopically low precipitation event, which occurred one week after the fire.

The post-fire decrease in drip water $\delta^{18}\text{O}$, associated with a convergence of drip water and precipitation d-excess, is attributed to the recharge from this post-fire precipitation event. No similar $\delta^{18}\text{O}$ or $\delta^2\text{H}$

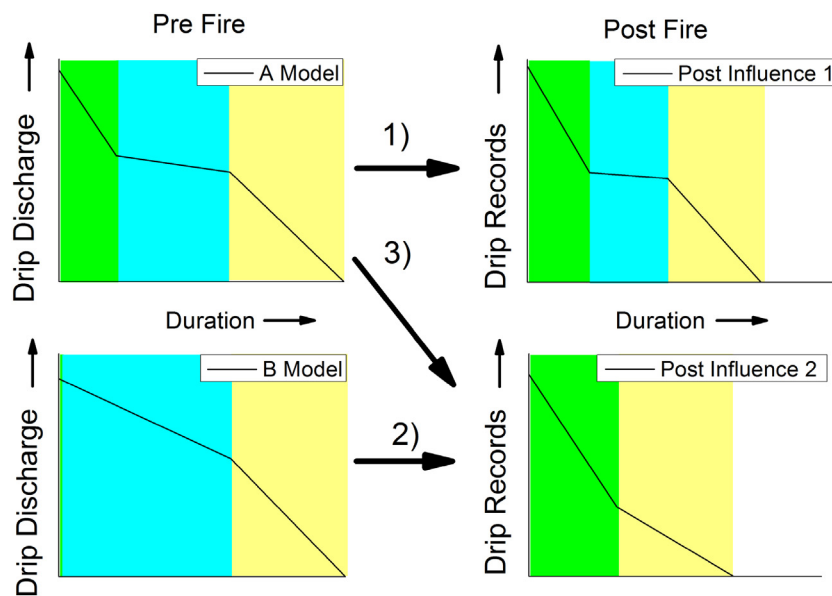


Fig. 7. Conceptual models for the fire influence on vadose zone discharge events during individual precipitation events. Y-axis is displayed in log10 transformation. Stages a in green represent the preferential flows dominated stage, b in blue the soil diffuse flows dominated stage, c in yellow the residual flows. A model indicates a drip pattern with notable soil diffuse flow stage, and B model indicates with extreme low soil preferential flow.

isotope excursions are observed in the drip waters in the pre-fire period (Fig. 4), although no equivalently large and isotopically anomalous precipitation events occurred over this time period (Supplemental Table 2). From our drip hydrology data we would infer a loss of soil capillarity and an increase in preferential flow after the fire, which might be expected to increase the magnitude of the drip water isotopic response to precipitation. Changes in the slopes of $\delta^2\text{H}$ vs $\delta^{18}\text{O}$ for drip waters pre and post fire, in comparison to the local meteoric water line, could help elucidate changes in soil and vadose zone residence time if drip waters were affected by evaporation, however results are inconclusive as observed changes in slopes are within their uncertainties (Fig. 6). Comparison of d-excess of drip water and precipitation shows that drip water d-excess returns to a higher value than precipitation at the end of the monitoring period, suggesting a return to pre-fire conditions by this time.

We therefore summarise that we do not see more positive isotopes as reported by Nagra et al. (2016), and attributed to increased evaporation and partial enrichment of soil water isotope due to evaporative fractionation. We hypothesise that for our experimental fire, whose severity was such that soil properties changed, that there was a complete evaporation of soil and shallow vadose zone water. Drip water isotopic compositions post-fire therefore represent the isotopic characteristics of the first recharge, and subsequent recharge events helped replenish the karst fractures and stores and soil water, whose isotopic composition gradually returns to an integrated mean of those event after 6 months.

5.3. Drip water solutes signatures

The hydrological interpretation indicates a decrease in water residence time, which is associated with decreased dissolution of bedrock and subsequent precipitation of calcite (Fairchild and Treble, 2009). Bedrock-related solutes including Ca^{2+} , Mg^{2+} and Sr^{2+} decreased one month post-fire (see Table 1). This could reflect a decrease in carbonate dissolution due to the evaporation of old storage water and a shorter water residence time. Decreased soil CO_2 from the destruction of plant roots and microbial communities could also enhance this effect.

Comparison of Mg/Ca and Sr/Ca ratios can be used as a geochemical signature of the amount of bedrock dissolution based on the prior calcite precipitation effects (Treble et al., 2003; Fairchild and Treble, 2009). These ratios did not show any notable differences between the pre- and post-fire groups within the study timescale (see Fig. 8). It suggests that, for this shallow cave, each precipitation event barely reached saturation for calcite before discharging into the cave. Within-cave evidence for this interpretation is abundant stalactite formations occurring without associated deposition of stalagmites.

Despite ash being present across the fire site, there was only limited geochemical evidence of ash-derived solutes in the drip waters. Sulfate drip water concentration significantly increased ten-fold one month after fire, whereas concentrations of analysed cations decreased after the fire experiment. The lack of a post-fire rise in ash-derived cations including K, Na and Fe that would be expected from ash production, could be due to the volatilisation of solutes at high temperatures (Bodí et al., 2014). The fire temperature exceeded 929°C in some areas (see Supplementary Fig. 1) which could volatilise organic compounds leaving white ash, which was observed at the experiment site (Fig. 1). Moreover, I^- and Cl^- concentrations both increased slightly, respectively, and I^- concentration increased significantly six months after the fire. Concentrations of Cl^- also indicated the removal of soil water by the fire. This agrees with limited saturation index values for calcite calculated from 6 drip activities, from 0.44 ± 0.13 pre-fire to 0.62 ± 0.17 post-fire.

In summary, the combustion of vegetation and soil fauna is hypothesised to lead to a decrease in limestone dissolution (lower Mg^{2+} , Ca^{2+} , and Sr^{2+} and a volatilisation in soil- and vegetation-derived solutes (K^+ , Na^+ , Si^{4+} , I^- and Fe^{2+}).

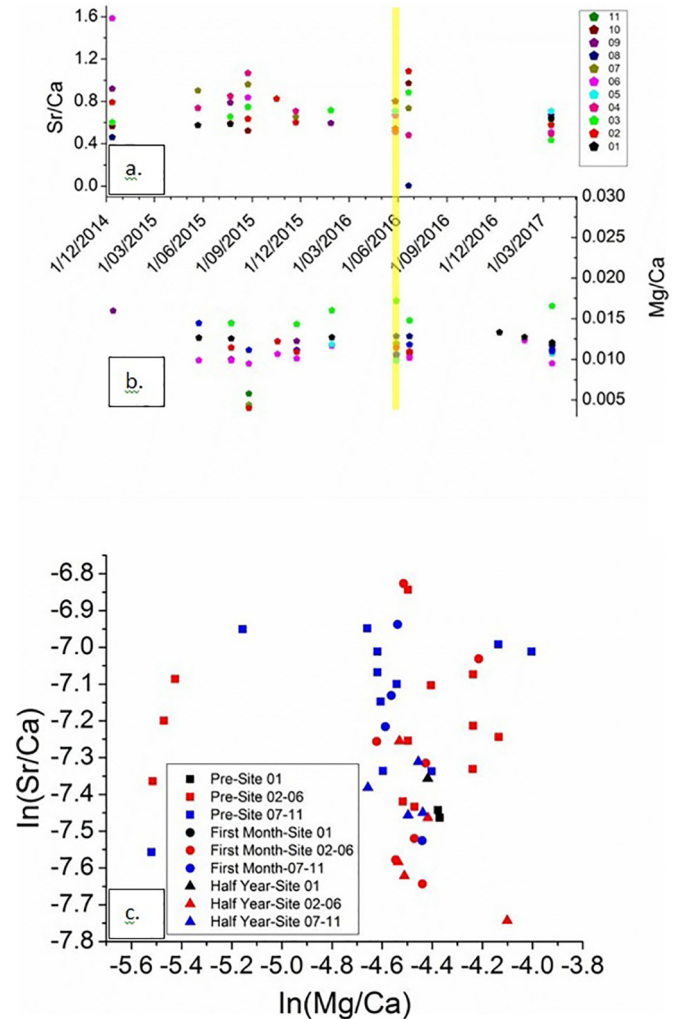


Fig. 8. Ratios of Sr/Ca (a), Mg/Ca (b), and $\ln(\text{Sr}/\text{Ca})$ vs $\ln(\text{Mg}/\text{Ca})$ (c). The vertical yellow line indicates the timing of the experimental fire (25th May 2016).

6. Conclusion

This research has demonstrated the impacts of a high-severity experimental fire on the karst vadose zone, including 1) short-term complete evaporation of soil water; 2) increased preferential flows and decreased soil diffuse flows; and 3) increased soil hydrophobicity. Three different stages of discharge: preferential flows dominated stage, soil diffuse flows dominated stage and residual flows dominated stage were defined based on the hydrograph analysis on the cave drip rates in this study. Based on that, a more intense stage 1 post fire was attributed to the increased preferential flows, and decreased stage 2 to the decreased importance of soil diffuse flow post fire.

The short-term responses observed in cave drip water isotopic and hydrochemical composition were large shifts in stable water isotope composition to lower values and decreased concentrations of bedrock-derived solutes within the first month post-fire. The lower isotopic values show that older pre-existing soil water with a higher isotopic value was removed by evaporation due to the heat of the fire. A shorter water residence time post fire resulted in relatively lower values with respect to $\delta^2\text{H}$ and $\delta^{18}\text{O}$. A post-fire return to a more enriched isotopic composition was observed.

The bedrock-related solute concentrations decreased after the fire experiment because of lower recharge durations and potentially

decreased partial pressure of carbon dioxide (pCO₂). Ash products were largely volatilised due to the severe intensity of the fire and were not captured by the cave, instead leaving white-coloured ash above the cave.

This study has demonstrated a potential explanation for the lower δ¹⁸O values in fire records which is opposite to the higher δ¹⁸O from increased albedo observed by Nagra et al. (2016), and provides evidences to utilise the decreased bedrock solutes as one important factor for paleo-fire tracing. If another fire experiment was conducted during dry season, a smaller change in the hydrological regime would be expected as antecedent soil moisture would already be low. In addition to this, similar nutrient solutes trends should be observed with similar fire volatilisation.

Acknowledgements

The research was partly funded by Australian Research Council Linkage LP13010017 and Land & Water Australia grant (ANU52) to Pauline Treble. The authors appreciate the efforts from team at Wombeyan Karst Conservation Reserve, especially David Smith, the manager for his support and assistance with logistics and accommodation. We thank Andy Spate and Sophia Meehan for overall project design for LP13010017. Martina De Marcos and Xiaolin Shan helped with in field work and Yuyan Yu with documents. Thank you to Bob Cullen for collecting rainfall samples at Mt. Werong, Barbara Gallagher and Jennifer van Holst (ANSTO) for analysis of rainfall samples, and the Sydney Catchment Authority for providing rainfall data. And the authors want to give special thanks to the anonymous reviewers from Science of the Total Environment, especially on the interpretations of fire influence.

Appendix A. Supplementary data

Supplementary data to this article can be found online at <https://doi.org/10.1016/j.scitotenv.2019.01.102>.

References

- Atkinson, T., 1977. Diffuse flow and conduit flow in limestone terrain in the Mendip Hills, Somerset (Great Britain). *J. Hydrol.* 35, 93–110.
- Baker, A., Barnes, W.L., Smart, P.L., 1997. Variations in the discharge and organic matter content of stalagmite drip waters in Lower Cave, Bristol. *Hydrol. Process.* 11, 1541–1555.
- Beven, K., Germann, P., 1982. Macropores and water flow in soils. *Water Resour. Res.* 18, 1311–1325.
- Bodí, M.B., Martín, D.A., Balfour, V.N., Santín, C., Doerr, S.H., Pereira, P., Cerdà, A., Mataix-Solera, J., 2014. Wildland fire ash: production, composition and eco-hydrogeomorphic effects. *Earth Sci. Rev.* 130, 103–127.
- Bonacci, O., Gottstein, S., Roje-Bonacci, T., Vuletić, J., 2008. Effects of wildfire on hydrology, erosion processes and ecology on karst environment: case of the island of Hvar (Croatia). EGU General Assembly.
- Brunker, R., Offenberg, A., 1970. Goulburn 1: 250 000 Geological Sheet. S155–12. New South Wales Geological Survey, Sydney.
- Coleborn, K., Rau, G.C., Cuthbert, M.O., Baker, A., Navarre, O., 2016a. Solar-forced diurnal regulation of cave drip rates via phreatophyte evapotranspiration. *Hydrol. Earth Syst. Sci.* 20, 4439.
- Coleborn, K., Spate, A., Tozer, M., Andersen, M.S., Fairchild, I.J., MacKenzie, B., Treble, P.C., Meehan, S., Baker, A., Baker, A., 2016b. Effects of wildfire on long-term soil CO₂ concentration: implications for karst processes. *Environ. Earth Sci.* 75, 1–12.
- Collister, C., Mathey, D., 2008. Controls on water drop volume at speleothem drip sites: an experimental study. *J. Hydrol.* 358, 259–267.
- Crawford, J., Hughes, C.E., Parkes, S.D., 2013. Is the isotopic composition of event based precipitation driven by moisture source or synoptic scale weather in the Sydney Basin, Australia? *J. Hydrol.* 507, 213–226.
- Cuthbert, M.O., Baker, A., Jex, C.N., Graham, P.W., Treble, P.C., Andersen, M.S., Acworth, R.L., 2014 Jun 1. Drip water isotopes in semi-arid karst: implications for speleothem paleoclimatology. *Earth Planet. Sci. Lett.* 395, 194–204.
- Fairchild, I.J., Baker, A., 2012. *Speleothem Science: From Process to Past Environments*. vol. 3. John Wiley & Sons.
- Fairchild, I.J., Treble, P.C., 2009. Trace elements in speleothems as recorders of environmental change. *Quat. Sci. Rev.* 28, 449–468.
- Fairchild, I.J., Borsato, A., Tooth, A.F., Frisia, S., Hawkesworth, C.J., Huang, Y., et al., 2000. Controls on trace element (Sr–Mg) compositions of carbonate cave waters: implications for speleothem climatic records. *Chem. Geol.* 166, 255–269.
- Fernandez, I., Cabaneiro, A., Carballas, T., 1999. Carbon mineralization dynamics in soils after wildfires in two Galician forests. *Soil Biol. Biochem.* 31, 1853–1865.
- Fredlund, D.G., Rahardjo, H., 1993. *Soil Mechanics for Unsaturated Soils*. Wiley, New York (517p).
- Froehlich, K., Kralik, M., Papesch, W., Rank, D., Scheifinger, H., Stichler, W., 2008. Deuterium excess in precipitation of Alpine regions—moisture recycling. *Isot. Environ. Health Stud.* 44, 61–70.
- Ghodrati, M., Jury, W.A., 1992. A field study of the effects of soil structure and irrigation method on preferential flow of pesticides in unsaturated soil. *J. Contam. Hydrol.* 11, 101–125.
- Gröning, M., Lutz, H., Roller-Lutz, Z., Kralik, M., Gourcy, L., Pöntenstein, L., 2012. A simple rain collector preventing water re-evaporation dedicated for δ¹⁸O and δ²H analysis of cumulative precipitation samples. *J. Hydrol.* 448, 195–200.
- Hartland, A., Fairchild, I.J., Lead, J.R., Borsato, A., Baker, A., Frisia, S., Baalousha, M., 2012. From soil to cave: transport of trace metals by natural organic matter in karst dripwaters. *Chem. Geol.* 304, 68–82.
- Haslem, A., Kelly, L.T., Nimmo, D.G., Watson, S.J., Kenny, S.A., Taylor, R.S., Avitabile, S.C., Callister, K.E., Spence-Bailey, L.M., Clarke, M.F., Bennett, A.F., 2011. Habitat or fuel? Implications of long-term, post-fire dynamics for the development of key resources for fauna and fire. *J. Appl. Ecol.* 48, 247–256.
- Huang, Y., Fairchild, I.J., 2001. Partitioning of Sr²⁺ and Mg²⁺ into calcite under karst-analogue experimental conditions. *Geochim. Cosmochim. Acta* 65, 47–62.
- Huffman, E.L., MacDonald, L.H., Stednick, J.D., 2001. Strength and persistence of fire-induced soil hydrophobicity under ponderosa and lodgepole pine. *Colorado Front Range. Hydrol. Process.* 15, 2877–2892.
- Hughes, C.E., Crawford, J., 2013. Spatial and temporal variation in precipitation isotopes in the Sydney Basin, Australia. *J. Hydrol.* 489, 42–55.
- Immenhauser, A., Dublyansky, Y.V., Verwer, K., Fleitman, D., Pashenko, S.E., 2007. Textural, elemental, and isotopic characteristics of Pleistocene phreatic cave deposits (Jabal Madar, Oman). *J. Sediment. Res.* 77, 68–88.
- Jouzel, J., Hoffmann, G., Koster, R., Masson, V., 2000. Water isotopes in precipitation: data/model comparison for present-day and past climates. *Quat. Sci. Rev.* 19, 363–379.
- Keeley, J.E., 2009. Fire intensity, fire severity and burn severity: a brief review and suggested usage. *Int. J. Wildland Fire* 18, 116–126.
- Kogovšek, J., 2010. Characteristics of percolation through the karst vadose zone. 10. Založba ZRC, Ljubljana 168p.
- Mann, H.B., Whitney, D.R., 1947 Mar. On a test of whether one of two random variables is stochastically larger than the other. *Ann. Math. Stat.* 1, 50–60.
- McDonald, J., Drysdale, R., 2007. Hydrology of cave drip waters at varying bedrock depths from a karst system in southeastern Australia. *Hydrol. Process.* 21, 1737–1748.
- Nagra, G., Treble, P.C., Andersen, M., Fairchild, I.J., Coleborn, K., Baker, A., 2016. A post-wildfire response in cave dripwater chemistry. *Hydrology and Earth System Sciences Discussions*.
- Osborne, R., 1984. Multiple karstification in the lachlan fold belt in New South Wales: reconnaissance evidence. *J. Proc. R. Soc. NSW* 107, 15–34.
- Osborne, R., 1993. The history of karstification at Wombeyan Caves, New South Wales, Australia, as revealed by palaeokarst deposits. *Cave Science* 20, 1–8.
- Pausas, J.G., Llovet, J., Rodrigo, A., Vallejo, R., 2009. Are wildfires a disaster in the Mediterranean basin?—a review. *Int. J. Wildland Fire* 17, 713–723.
- Plaza-Álvarez, P.A., Lucas-Borja, M.E., Sagra, J., Moya, D., Alfaro-Sánchez, R., González-Romero, J., et al., 2018. Changes in soil water repellency after prescribed burnings in three different Mediterranean forest ecosystems. *Sci. Total Environ.* 644, 247–255.
- Razowska-Jaworek, L., 2014. *Calcium and Magnesium in Groundwater: Occurrence and Significance for Human Health*. CRC Press, Boca Raton, America (236pp).
- Russo, D., 1998. Stochastic analysis of flow and transport in unsaturated heterogeneous porous formation: effects of variability in water saturation. *Water Resour. Res.* 34, 569–581.
- Scott, D., Van Wyk, D., 1990. The effects of wildfire on soil wettability and hydrological behaviour of an afforested catchment. *J. Hydrol.* 121, 239–256.
- Šimúnek, J., Jarvis, N.J., Van Genuchten, M.T., Gårdenäs, A., 2003. Review and comparison of models for describing non-equilibrium and preferential flow and transport in the vadose zone. *J. Hydrol.* 272, 14–35.
- Smart, P., Friederich, H., 1987. Water movement and storage in the unsaturated zone of a maturely karstified aquifer, Mendip Hills, England. Proceedings, Conference on Environmental Problems in Karst Terrains and their Solution, Bowling Green, Kentucky. National Water Well Association, pp. 57–87.
- Sophocleous, M., 2002. Interactions between groundwater and surface water: the state of the science. *Hydrobiol.* J. 10, 52–67.
- Soulsby, C., Malcolm, R., Helliwell, R., Ferrier, R., Jenkins, A., 2000. Isotope hydrology of the Allt a'Mharcaidh catchment, Cairngorms, Scotland: implications for hydrological pathways and residence times. *Hydrol. Process.* 14, 747–762.
- Stoof, C.R., Slingerland, E.C., Mol, W., Berg, J., Vermeulen, P.J., Ferreira, A.J., Ritsema, C.J., Parlange, J.Y., Steenhuis, T.S., 2014. Preferential flow as a potential mechanism for fire-induced increase in streamflow. *Water Resour. Res.* 50, 1840–1845.
- Ternan, J.L., 1972. Comments on the use of a calcium hardness variability index in the study of carbonate aquifers: with reference to the central Pennines, England. *J. Hydrol.* 16, 317–321.
- Tian, L., Yao, T., MacClune, K., White, J.W., Schilla, A., Vaughn, B., Vachon, R., Ichiyangi, K., 2007. Stable isotopic variations in west China: a consideration of moisture sources. *J. Geophys. Res.-Atmos.* 112, D10.
- Treble, P., Shelley, J.M.G., Chappell, J., 2003. Comparison of high resolution sub-annual records of trace elements in a modern (1911–1992) speleothem with instrumental climate data from southwest Australia. *Earth Planet. Sci. Lett.* 216, 141–153.
- Treble, P.C., Fairchild, I.J., Baker, A., Meredith, K.T., Andersen, M.S., Salmon, S.U., Bradley, C., Wynn, P.M., Hankin, S.I., Wood, A., McGuire, E., 2016. Roles of forest bioproductivity,

- transpiration and fire in a nine-year record of cave dripwater chemistry from south-west Australia. *Geochim. Cosmochim. Acta* 184, 132–150.
- Tremaine, D.M., Froelich, P.N., 2013. Speleothem trace element signatures: a hydrologic geochemical study of modern cave dripwaters and farmed calcite. *Geochim. Cosmochim. Acta* 121, 522–545.
- Wassenaar, L., Terzer-Wassmuth, S., Douence, C., Araguas-Araguas, L., Aggarwal, P., Coplen, T.B., 2018. Seeking excellence: an evaluation of 235 international laboratories conducting water isotope analyses by isotope-ratio and laser-absorption spectrometry. *Rapid Commun. Mass Spectrom.* 32, 393–406.
- Wassenburg, J.A., Immenhauser, A., Richter, D.K., Jochum, K.P., Fietzke, J., Deininger, M., Goos, M., Scholz, D., Sabaoui, A., 2012. Climate and cave control on Pleistocene/Holocene calcite-to-aragonite transitions in speleothems from Morocco: elemental and isotopic evidence. *Geochim. Cosmochim. Acta* 92, 23–47.
- White, W.B., 2002. Karst hydrology: recent developments and open questions. *Eng. Geol.* 65, 85–105.
- Wylie, J., Wylie, G., 2004. The caves of Wombeyan: an annotated listing. *Caves and Karst of Wombeyan*. 13. Sydney Speleological Society Occasional Paper, pp. 167–196.